HHS Public Access

Author manuscript

Brain Res. Author manuscript; available in PMC 2020 November 15.

Published in final edited form as:

Brain Res. 2019 November 15; 1723: 146378. doi:10.1016/j.brainres.2019.146378.

Cholesterol Sulfate Alters Astrocyte Metabolism and Provides Protection Against Oxidative Stress

Jude Prah, **Ali Winters**, **Kiran Chaudhari**, **Jessica Hersh**, **Ran Liu**, **Shao-Hua Yang**

Department of Pharmacology and Neuroscience, Institute for Healthy Aging, University of North Texas Health Science Center, Fort Worth, TX 76107, USA

Abstract

Cholesterol sulfate (CS) is one of the most important known sterol sulfates in human plasma and it is present as a normal constituent in a variety of human tissues. In both the brain and periphery, CS serves as a substrate for the synthesis of sulfonated adrenal steroids such as pregnenolone sulfate and dehydroepiandrosterone (DHEA) sulfate and as a constituent of many biological membranes including red blood cells where it functions as a stabilizing agent. It also acts as an endogenous regulator of cholesterol synthesis. However, the role of CS in brain metabolism and neurological disorder is unclear. In the current study we investigated the neuroprotective action of CS as well as its role in brain energy metabolism. The neuroprotective effect of CS and its role on cell metabolism were determined in primary astrocyte prepared from the cortex of postnatal day 0–2 C57BL/6 pups and a hippocampal HT-22 cell line using Calcein AM and MTT cell viability assay, flow cytometry, Seahorse extracellular flux analysis, and metabolism assay kits. We found that CS attenuates glutamate and rotenone induced cell death in HT-22 cells, decrease glutamate induced mitochondria membrane potential collapse, and reactive oxygen species production. Additionally, CS activates the Akt/Bcl_2 pathway. We observed that CS impacts astrocyte metabolism by increasing mitochondrial phosphorylation, ATP, and glycogen contents. Our study demonstrated that CS modulates brain energy metabolism and its neuroprotective effects might be due to the activation of Akt signaling or its ability to decrease reactive oxygen species production.

Keywords

Cholesterol sulfate; Neuroprotection; Astrocytes; metabolism; oxidative stress

1. Introduction

Cholesterol sulfate (CS) is a major known sterol sulfate in human plasma with its concentration ranging from 135 to 260 μg/ml (Shi et al., 2014; Strott & Higashi, 2003). CS

#**Corresponding Author:** Shao-Hua Yang, M.D., Ph.D. Department of Pharmacology and Neuroscience University of North Texas Health Science Center 3500 Camp Bowie Boulevard Fort Worth, TX 76107 817-735-2250 (Fax: 817-735-2091), shaohua.yang@unthsc.edu.

is distributed in seminal fluid, urine, adrenal glands, liver, hair, nails and uterine endometrium (Nakae et al., 2010; Sion, Grizard, & Boucher, 2001; Strott & Higashi, 2003; Winter & Bongiovanni, 1968). CS plays an important role in cell membrane stabilization, cell adhesion, and protection against osmotic induced cell lysis (Strott & Higashi, 2003). Additionally, it has been demonstrated that CS is an inhibitor of gluconeogenesis in hepatocytes and play a role in sterologenesis in human Keratinocytes and Fibroblasts (Shi et al., 2014; Williams, Hughes-Fulford, & Elias, 1985). CS deficiency has been proposed to be involved in the development of atherosclerosis (Seneff, Davidson, Lauritzen, Samsel, & Wainwright, 2015). In the brain, CS has been reported to be significantly high in the cerebellum compared to other regions, although the specific cerebellum associated role remains undefined (Ivanisevic serves et al., 2014). In addition, CS serves as a substrate for the synthesis of pregnenolone sulfate and dehydroepiandrosterone (DHEA) sulfate, major neurosteroids that affect many neuronal functions (Hochberg, Ladany, Welch, & Lieberman, 1974; Roberts, Bandi, Calvin, Drucker, & Lieberman, 1964). However, the role of CS in brain metabolism and neurological disorder is unclear.

Astrocytes, the most abundant glial cells in the CNS, are critical in maintaining CNS homeostasis. Astrocytes play an important role in clearance and metabolism of neurotransmitters, regulation of extracellular ions, blood-brain barrier formation, synaptic transmission regulation, and controlling local blood flow (Belanger & Magistretti, 2009; Sofroniew & Vinters, 2010). Astrocytes play an active role in brain energy production, storage, and utilization to meet the metabolic demands of neuron via astrocyte-neuron metabolic coupling (Belanger, Allaman, & Magistretti, 2011). In addition, astrocytes have been suggested to play a critical role in brain cholesterol metabolism. It has been widely accepted that energy metabolism plays a fundamental role in the pathogenesis of many neurodegenerative diseases and energy metabolism could be a potential target in the prevention and treatment of neuropathologies (Johnson & Imai, 2018; Quansah et al., 2018). Similarly, impairments in astrocyte metabolism have been linked to neurodegenerative processes (Maragakis & Rothstein, 2006). The goal of this study was to test the hypothesis that CS alters brain bioenergetics and offers protection against oxidative insult. This is based on several studies which demonstrated the role of CS as a substrate for the synthesis of neurosteroids which display neuroprotective properties (Borowicz, Piskorska, Banach, & Czuczwar, 2011).

2. Results

2.1. CS protects HT-22 cells against glutamate and rotenone induced cell death

The protective effects of CS were characterized in HT-22 cells against glutamate, glucose oxidase, and rotenone insults. The cells were either pre-treated with CS for 24 or 36 hours before being exposed to glutamate for 12 hours or treated with CS in the presence of glutamate or rotenone. In both Calcein AM and MTT assay, CS dose-dependently protected HT-22 cells against glutamate-induced cell death in both pre- and co-treatment paradigms (Figure 1A and B). Florescent images of HT-22 cells stained with Calcein AM and propidium iodide (PI) also showed that CS increased cell viability when the cells were exposed to a toxic dose of glutamate (Figure 1C). In the Calcein AM assay, CS protected

HT-22 cells with an EC50 of 17.6 μM when the cells were co-treated with CS and glutamate for 12 hours (Figure 1D). When HT-22 cells were pre-treated with CS for 24 and 36 hours before glutamate induced cell death, CS increased cell viability with an EC50 of 22.6 μM and 11.4 μM, respectively (Figure 1D). Flow cytometry of annexin V and PI staining of HT22 cells exposed to glutamate for 12 hours showed that 9.64%, 14.1%, and 48.2% of cells were in the early, late and necrotic stages of cell death, respectively, which were significantly decreased to 1.54%, 2.38%, and 22.8%, respectively, when pre-treated with CS for 24 hours (Figure 1E). Similarly, co-treatment of 30 and 50 μM CS significantly decreased rotenone-induced cell death (Figure 2A). Interestingly, CS failed to protect HT-22 cells against toxic doses of glucose oxidase (Figure 2B).

The effect of CS on glutamate-induced ROS generation was measured using fluorescent indicator H_2DCFDA which is converted into DCF by ROS. Flow cytometry assay revealed that glutamate caused a significant increase in ROS which was attenuated by co-treatment of CS (Figure 3A). The inhibitory action of CS on ROS generation in HT-22 cells was also verified using a microplate reader. CS significantly decreased ROS production measured as total cellular ROS (Figure 3B). Treatment of HT-22 cells with glutamate caused a loss of mitochondrial membrane potential evidenced by TMRE microplate reader analysis which was attenuated by treatment of CS (Figure 3C).

We investigated the effects of CS on glutamate-induced GSH depletion and observed that CS dose-dependently inhibited glutamate-induced loss of GSH (Figure 4A). The effects of CS on the activity of superoxide dismutase, an enzyme that converts superoxide radicals to hydrogen peroxide and molecular oxygen (Weydert & Cullen, 2010) was measured. We observed that CS does not affect SOD activity (Figure 4B). We determined the effect of CS on the Akt anti-apoptotic pathway. HT-22 cells were treated with CS for 36 hours. Western blot analysis showed that CS dose-dependently increased Akt phosphorylation and increased Bcl-2/Bax ratio (Figure 5A and B).

2.2. CS increased ATP content, glycogen storage and mitochondrial respiration in astrocytes

The effects of CS on astrocyte metabolism were determined using a Seahorse XFe 96 analyzer. We measured parameters of oxygen consumption rate (OCR) such as basal and maximal respiration, ATP-linked respiration, non-mitochondrial respiration, proton leak, and extracellular acidification rate (ECAR) before and after sequential injection oligomycin, FCCP, and Rotenone/Antimycin A. After 72 hour treatments of astrocytes with different concentrations of CS we observed that 50 μM CS increased basal and maximal respiration, spare respiratory capacity, and ATP production linked to OCR (Figure 6A). We also observed an increase in non-mitochondrial respiration, a parameter of OCR (Figure 6A). No significant increase was observed in the extracellular acidification rate in astrocytes treated with CS for 72 hours and the cell energy metabolic phenotype shifted toward mitochondrial oxidative phosphorylation upon CS treatment (Figure 6B). A similar effect was also observed in CS-treated HT-22 cells (Supplementary Figure 1). We determined the effects of CS on ATP levels in astrocytes. CS significantly increased total ATP content after astrocytes (Figure 7A) and HT-22 (Supplementary Figure 2) was treated with CS for 72 hours and

lactate levels in the astrocyte culture media (Figure 7B). Furthermore, increased glycogen (Figure 7C) and lipid content (Figure 7D) in astrocyte was observed after CS treatment.

2.3. CS increased AMPK activation

We determined the effects of CS on the AMPK pathway in primary astrocytes. Western blot analysis indicated that 72-hour treatment of CS significantly decreased phosphorylation of AMPKα (Figure 8A) while increased mTOR phosphorylation in primary astrocyte cultures (Figure 8A). Consistently, decreased phosphorylation of Acetyl-CoA (ACC) and glycogen synthase (GS) were observed in primary astrocytes upon CS treatment (Figure 8B).

3. Discussion

Neuroprotective strategies are aimed at protecting and preserving the CNS cell's structure and function from insults arising from toxins and neurodegenerative diseases. Several cellular mechanisms are involved in the initiation and progression of events leading to CNS cell structure and functional loss. This includes mitochondrial dysfunction, excitotoxicity, defects in energy metabolism, and oxidative stress (Belanger & Magistretti, 2009; Blaszczyk, 2018; Reynolds, Laurie, Mosley, & Gendelman, 2007). ROS production facilitates a vicious cycle of accelerated excitotoxity, lipid peroxidation, accelerated mitochondrial damage, and inflammation leading to neuronal loss (Guo, Sun, Chen, & Zhang, 2013; Nita & Grzybowski, 2016). Oxidative stress also plays an important role in cognitive impairment caused by normal aging and neurodegenerative diseases (Silva et al., 2004). In this current study, we investigated the neuroprotective role of CS in HT-22 cells using various *in vitro* neurotoxic models.

Our study demonstrated that CS protected HT-22 cells against glutamate and rotenone-induced cell death. Treatment of CS decreased glutamate-induced increase of total ROS levels, mitochondrial membrane potential collapse, and rescued cells from apoptosis. In HT-22 cells glutamate blocks the glutamate/cysteine antiporter with saturating concentrations of extracellular glutamate resulting in glutathione (GSH) depletion leading to cell death (Fukui, Song, Choi, Choi, & Zhu, 2009; Murphy, Miyamoto, Sastre, Schnaar, & Coyle, 1989). Our data indicated that CS prevents glutamate-induced GSH depleting. AKT and its target B cell lymphoma-2 (Bcl-2) have been recognized as an anti-apoptotic factor (Franke, Hornik, Segev, Shostak, & Sugimoto, 2003; Zhou, Li, Meinkoth, & Pittman, 2000) In our study, we observed that CS significantly increased AKT phosphorylation as well as increased the expression of Bcl2 with no significant change in Bax expression. Our data suggest that the anti-apoptotic effect of CS in the presence of glutamate could be attributed to its ability to increase anti-apoptotic factors. Interestingly *in vivo* and *in vitro* studies have shown that many neurosteroids have neuroprotective effects. For instance DHEA, DHEAS, and progesterone have been shown to protect hippocampal neurons against glutamate-induced neurotoxicity (Wojtal, Trojnar, & Czuczwar, 2006). DHEA and DHEAS neuroprotective effects have been attributed to its anti-apoptotic effect via AKT/Bcl-2 pathway (Charalampopoulos et al., 2004; Yousefi et al., 2018; Zhernova & Ivanova, 2012). Since cholesterol sulfate serves as a substrate for the synthesis of DHEAS, it is possible that

the neuroprotective effects of CS observed could be because CS is converted to DHEAS by the cells *in vitro*.

Astrocytes play a critical role in glucose metabolism to ensure adequate energy substrate delivery to neurons in accordance with brain activity (Belanger et al., 2011). In addition, astrocytes are the major site of lipid metabolism in the brain which is tightly regulated to maintain neuronal structure and function. AMPK regulates energy metabolism under physiological and pathological conditions in the brain. It is activated by conditions that compromise cellular ATP or increase ATP consumption whereas high ATP concentration antagonizes AMPK activation (Cai et al., 2016). In our study, we observed that CS increased astrocyte ATP production and inhibited AMPK pathway. Glucose metabolism and ATP generation occur in a compartmentalized way in the brain. Whereas astrocytes rely heavily on glycolytic metabolism, neurons use the end products of glycolysis for oxidative metabolism (Belanger et al., 2011; Halim et al., 2010). Interestingly our cellular bioenergetics analysis indicates that CS significantly increases the mitochondrial oxygen consumption rate but has no effect on extracellular acidification rate although we observed an increase in lactate production by the cells. We expect that the increase in ATP production is likely due to the increased OCR as a result of CS-induced increase mitochondrial efficiency. Consistent with the inhibition of AMPK we observed an increase in lipogenesis and glycogenesis evident by decreased inactivation of ACC and GS. Glycogen a polymer of glucose is exclusively localized in astrocytes in the adult brain. It has been reported that almost half of the brain's glucose is taken up by astrocytes under physiological condition. It has been demonstrated that increasing astrocytic glycogen stores preserves the neuronal function and viability under limited conditions of restricted ATP availability, such as in hypoglycemia (Belanger et al., 2011; Brown et al., 2005; Swanson & Choi, 1993). We found a significant increase in glycogenesis in astrocytes following CS treatment indicated by the decrease in phosphorylated GS and increased glycogen content. The enhancement of glycogen stores and glycogenesis might also contribute to the increase in ATP production, and OCR observed following CS treatment. We speculate that CS activation of glycogen synthesis and increase ATP production might mediate the neuroprotective effect.

There have been conflicting reports about the physiological concentration of Cholesterol sulfate in human plasma. Utilizing different methodologies in large group subject, The concentration of plasma CS ranged between 135 to 260 μg/ml (Shi et al., 2014; Strott & Higashi, 2003), which is approximately 289 μM to 557 μM. However in limited number of subjects the concentrations of CS in the plasma range between 174 to 328 μg/100 ml which is approximately 4 μM to 7 μM (Bleau, Chapdelaine, & Roberts, 1972; Winter & Bongiovanni, 1968). Since the amount of CS in the brain have not been determined in human subjects but that in rat brain ranges between 17 to 50 μg/g dry weights, we first did a dose response assay as shown in figure 1D, base on which the doses of CS were chosen in the cell culture model.

In summary, our current study demonstrates that the CS protected HT-22 cells against glutamate-induced cell death. In addition, CS enhanced mitochondrial oxidative phosphorylation and increases energy storage in primary astrocytes. Further, *in vivo* studies

are needed to investigate the effects of CS on aging and other neurodegenerative disorders associated with oxidative stress and metabolic syndrome.

4. Materials and experimental procedure

4.1. Materials and Reagents

5'AMP-activated protein kinase (AMPK) (monoclonal, cell signaling), Glycogen synthase (GS) and Acetyl CoA Carboxylase (ACC) (Monoclonal Cell, signaling), mammalian target of rapamycin (mTOR) (monoclonal, cell signaling), Actin and GAPDH (monoclonal, Santa Cruz) as well as secondary antibodies from Jackson laboratory (USA) were used for western blot. Cell culture dishes, 24 well plates, 12 well plates, and 40 μM cell strainers were all purchased from Greiner bio-one (USA). In addition, 6 and 96 well plates were purchased from Genesee scientific (USA). L-Glutamic acids, Trypsin-EDTA, trypan blue and poly-L-Lysine solution were purchased from Sigma Aldrich (USA). Penicillin-streptomycin, sodium pyruvate, TrypLE, and glutmax were purchased from Gibco/life technologies (USA). Cholesterol sulfate was purchased from Cayman chemical (USA). Dulbecco's Modified Eagle's Medium (DMEM; Hyclone, USA) high and low glucose were used to culture the cells for the experiments.

4.2. Primary astrocyte culture

The institutional animal care and use committee of the University of North Texas Health Science Center UNTHSC approved all procedures performed during the isolation or preparation of primary astrocytes from C57BL6 mouse (Jackson's lab). As previously described (Roy Choudhury et al., 2015) primary astrocytes were prepared from 1-day old C57BL6 pups. Briefly, hypothermia was used to anesthetize day old C57BL6 mouse pups followed by decapitation with a sharp surgical scissor. The cerebral cortices were dissected and meninges removed under aseptic conditions. TrypLE was used to digest the cortices at 37 °C for 15 minutes with shaking after every 5mins. A single cell suspension was prepared by pipetting through 3 different sized pipettes after which the cell suspension was strained through 40 μM size cell strainer. The cells were counted and plated in a culture dish in Dulbecco's Modified Eagle's medium (DMEM with 5.5 mM glucose, 4 mM L-glutamine, 1mM sodium pyruvate, thermos scientific) containing charcoal-stripped 10 % fetal bovine serum and streptomycin (100 units/ml) - penicillin (100 μg/ml) and allowed to attach for 15 minutes in a humidified incubator at 37 °C with 5% CO_2 after which media was changed. When the cells became 80% confluent; the plates were constantly shaken for 24 hours in a CO_2 incubator at 37°C to eliminate microglia and other cell debris.

4.3. HT-22 Cell Culture

A murine hippocampal cell line HT-22 cells were maintained in high glucose Dulbecco's Modified Eagle Medium (DMEM) supplemented with charcoal-stripped 10% fetal bovine serum, 1 mM pyruvate and 4 mM glutamine in addition to streptomycin (100 units/ml) - penicillin (100 μg/ml) in tissue culture dishes. The cells were incubated at 37 °C under 5% CO_2. The medium was changed two times weekly, and cells split at confluence. The cells were used between passages 10 to 25.

Our lab have been using HT-22 cell line extensively to characterize the neuroprotective effects of many compounds against oxidative stress (Lin, Li, Winters, Liu, & Yang, 2018; Poteet et al., 2012). This cell line has also been characterized extensively by other groups. In HT22 cells, glutamate blocks glutamate/cysteine antiporter resulting in glutathione (GSH) depletion and cell death (Fukui et al., 2009; Murphy et al., 1989). Therefore, we used the HT-22 cell line to determine the antioxidative effect of CS.

4.4. Neuroprotective analysis

Cell viability assay—The ability of cholesterol and CS to protect cells against glutamate, rotenone and glucose oxidase induced cell death was assessed using different methods as previously described (Poteet et al., 2012). Briefly, HT-22 cells were washed with PBS and trypsinized to collect and count the cells. Three thousand cells/well were seeded in 96 well plates in 100 μl of DMEM (25 mM glucose, 1 mM pyruvate and 10% charcoal strip FBS) and allowed to attach for 6 hours at 37 °C with 5% CO_2. The cells were either pretreated with varying concentrations of CS for 12, 24 and 36 hours or the cells were co-treated with cholesterol sulfate, and neurotoxic substances. Cell death was induced with the following treatment: 20 mM glutamate for 12 hours, 5 μM rotenone treatments for 24 hours, and 2 U glucose oxidase treatments for 2 hours. Hours after treating the cells and incubating them at 37°C with 5% CO_2, MTT assay or Calcein AM viability assay was done using a microplate reader. For the MTT assay, plates were removed from the incubator, and 20 μl of 5 mg/ml MTT in PBS was added per well and returned into the incubator for 2 hours after gentle agitation. After 2 hours, the media was removed and 100 μl of DMSO was added to each well. Absorbance was measured at 560 nm with a reference of 670 nm on a Tecan Infinite F200 plate reader. For the Calcein AM assay the media was replaced with 1 μM solution of Calcein AM in PBS. The cells were then incubated at 37 °C for 5 minutes, and fluorescence was measured using a Tecan plate reader (excitation 485 emission 530). For fluorescent microscopy, following cell co-treatment with compounds and 20 mM glutamate for 12 hours, cells were incubated at 37°C in PBS containing 1 μg/ml Calcein AM and 5 μg/ml PI (BD Bioscience) for 15 minutes after which images were taken using Zeiss Observer Z1 microscope.

Apoptosis Analysis.—70,000 HT-22 cells/well were seeded in a 6 well plate and incubated overnight in 1 ml of DMEM (25 mM glucose, 1 mM pyruvate and 10% FBS) at 37°C with 5% CO_2. Varying concentrations of cholesterol sulfate and 20 mM glutamate were added to each well and incubated for 12 hours at 37°C with 5% CO_2. After 12 hours, both floating and attached cells were collected and cell apoptosis was analyzed using flow cytometry (BD LSR II, San Jose, CA, USA) following annexin–V and propidium iodide staining (BD Bioscience) according to the manufacturer's protocol. During apoptosis the membrane phospholipid phosphatidylserine (PS) is translocated to the outer surface of the plasma membrane binding Annexin V. Annexin V and Propidium iodide (PI) are used to indicate early and late apoptotic cells. Cells that are considered viable or live cells are both Annexin V and PI negative (Q4= % Annexin V^-/PI^-), while cells that are in early apoptosis are Annexin positive and PI negative (Q3= % Annexin V^+/PI^-), and cells that are in late apoptosis are both Annexin V and PI positive (Q2= % Annexin V^+PI^+), and cells are already dead are Annexin negative and PI positive (Q1= % Annexin V^-PI^+).

Reactive oxygen species (ROS) analysis—ROS fluorescent indicator H2DCFDA (Anaspec) was used to examine changes in reactive oxygen species using a fluorescent microplate reader and flow cytometry as previously described (Poteet et al., 2012). HT-22 cells were seeded at a density of 70,000 cells/well in a 6 well plate to attach overnight. Cells were treated with different concentrations of cholesterol sulfate, and then 20 mM glutamate and incubated for 12 hours at 37°C with 5% CO_2. 10 μM H2DCFDA in PBS was added to cells for 15 minutes, after which PBS containing H2DCFDA was replaced with fresh PBS, and the DCF fluorescence was determined with a Beckman Coulter FC-500. For the fluorescent microplate reader, HT-22 cells were seeded at a density of 3000 cells/well and incubated overnight in a 96 well plate containing 100 μl of DMEM (25 mM glucose, 1 mM pyruvate and 10% FBS) at 37 °C with 5% CO_2. Varying concentrations of CS and 20 mM glutamate were added to each well and incubated for 12 hours at 37°C with 5% CO_2. The cells were then incubated in PBS containing 10 μM H2DCFDA for 45 minutes at 37 °C and KRH for an additional 15 minutes. DCF florescence was measured using a Tecan Infinite F200 plate reader (excitation 485, emission 530) after washing the cells with PBS.

Mitochondrial membrane potential analysis—Mitochondrial membrane potential was examined using a fluorescent microplate reader as previously described (Lin et al., 2018). HT-22 cells were seeded in a 12 well plate at a density of 20,000 cells/well in DMEM (high glucose, 1 mM pyruvate and 10% FBS) overnight to attach. Cells were treated with different concentrations of CS and 20 mM glutamate after which cells were incubated for 8 hours at 37°C with 5% CO_2. Media was then replaced with PBS containing 1 μM Tetramethylrhodamine, Ethyl Ester (TMRE) working solution (Abcam, USA) for 20 min at 37 °C. Florescence intensity was measured using a Tecan Infinite F200 plate reader (Excitation 594, emission 575).

Super oxide dismutase and Glutathione Assay—HT-22 cells were seeded at a density of 70,000 cells/well in a 6 well plate and allowed to attach overnight. Cells were treated with different concentrations of CS for 24 hours and 20 mM glutamate for 12 hours. Super oxide dismutase (SOD) activity and GSH was measured using assay kits (Sigma Aldrich) according to the manufacturer's protocol.

4.5. Cell metabolism assays

Extracellular flux analysis—These experiments were conducted using both HT-22 cells and primary astrocytes. Oxygen consumption rate (OCR) and extracellular acidification rate (ECAR) was monitored using a Seahorse Bioscience XFe96 Extracellular Flux Analyzer as previously described (Prah et al., 2019). Astrocytes were seeded in 96 well seahorse microplates with DMEM (low glucose for astrocytes and high glucose for HT-22, 1 mM pyruvate and 10% FBS) and were treated with different concentrations of CS for 72 hours. On the day of the experiment, the culture media was replaced with XF base media (supplemented with 1 mM pyruvate, 2 mM glutamine and 5.5 mM glucose adjusted to pH 7.4) and incubated for 1 hour in a non-CO_2 incubator at 37°C. Rotenone/Antimycin A, FCCP, and oligomycin were diluted into the XF base media and loaded into the accompanying cartridge to achieve final concentrations of 0.5 μM, 1 μM, and 1 μl, respectively. Initial baseline readings were established followed by injections of the drugs

into the medium at the time points specified. For cell energy phenotype determination, oligomycin and FCCP was diluted in XF medium together to achieve a final concentration of 1 μM oligomycin and 1 μM FCCP and loaded into one port. Various metabolic parameters were monitored with each cycle set as mix for 3 minutes, delay for 2 minutes, and then measure for 3 minutes. Values were normalized to the cell number of each well determined by Calcein AM assays.

ATP and NAD/NADH assay—Astrocytes were plated and allowed to attach for 2 days at 37 °C and CO_2. The cells were then treated with different concentrations of CS for 72 hours. ATP concentrations in cell lysates were determined using an ATP determination Kit (Invitrogen USA) according to the manufacturer's protocol. Briefly, cells were washed with PBS and lysed with ATP releasing buffer (500 mM Tricine buffer, pH 7.8, 100 mM MgSO4, 2 mM EDTA, and 2 mM sodium azide, 1% Triton X-100). ATP standards and 10 μl of cell lysate were added to a 96 well plate after which 100 μl of ATP reaction buffer was added to each well. Luminescence was immediately determined using a Tecan Infinite F200 plate reader. Total ATP levels were normalized to protein content of the samples determined using Pierce 600 nm Protein assay (600 nm absorbance).

Glycogen assay—Total glycogen in astrocytes following treatment of the cells with different concentrations of CS for 72 hours was determined. Briefly, astrocytes were collected using 0.25% trypsin (Sigma) to detach the cells, washed twice with PBS, and resuspended in distilled water. Glycogen assay kits (Sigma-Aldrich, St Louis, MO) were used to measure glycogen content according to the manufacturer's manual. Glycogen levels were normalized to the protein concentration of each sample.

Lipid analysis—Lipid content was analyzed using Nile red staining. Propranolol that is known to induce accumulation of phospholipids and cyclosporine A that induces formation of prominent neutral lipid droplets as previously described (Grandl & Schmitz, 2010) were used as positive controls in the experiments. Astrocytes were treated with different concentrations of CS and 60 μM propranolol and cyclosporine for 72 hours. The cells were fixed with 10% formalin for 15 minutes at room temperature and stained with PBS containing 1 μM Nile red solution and 5 μg/ml Hoechst 33342 for 30 minutes. Florescence was measured using a Tecan Infinite F200 plate reader at various wavelengths: Neutral lipid droplets 488/560, phospholipids 532/>620, Hoechst 33342; 361/486. Values of fluorescence were normalized to those of Hoechst fluorescence to control for cell number. Flow cytometry analysis was also done after staining the cells with Nile red.

4.6. Western Blot

Cells were collected and lysed in RIPA buffer (50 mM of Tris. HCl, pH 7.4,150 mM NaCl, 1mM EDTA, 1%Triton X) with protease and phosphatase inhibitors. Protein assay reagent Pierce 660 nm (Thermo Scientific) was used to determine the protein content of the samples. Protein lysate was run in polyacrylamide gel and transferred to a nitrocellulose membrane. After blocking for 1 hour, nitrocellulose membranes were incubated with primary antibodies: AMPKα and AMPKβ, GS and ACC, mTOR, Blc2, Akt, Actin overnight. The membranes were then incubated with horseradish peroxidase-conjugated secondary antibody

for 2 hours at room temperature. Using biospectrum 500 UVP imaging system, chemiluminescence signals were detected and protein densities analyzed.

4.7. Statistical analysis

All data are presented as the mean ± S.E.M. The significance of differences among groups with one independent variable was determined by one-way ANOVA with Bonferroni's correction for pairwise comparisons between groups when significance was detected. The significance of differences among groups where two independent variables were present was determined by two-way ANOVA with Bonferroni post-hoc test for planned comparisons between groups when significance was detected. For all tests, $p < 0.05$ (*) was considered significant.

Supplementary Material

Refer to Web version on PubMed Central for supplementary material.

Acknowledgments

This work was partly supported by National Institutes of Health grants R01NS088596 (SY) and R01NS109583 (SY); and American Heart Association Grant 17POST33670981 (KC).

REFERENCES

Belanger M, Allaman I, & Magistretti PJ (2011). Brain energy metabolism: focus on astrocyte-neuron metabolic cooperation. Cell Metab, 14(6), 724–738. doi:10.1016/j.cmet.2011.08.016 [PubMed: 22152301]

Belanger M, & Magistretti PJ (2009). The role of astroglia in neuroprotection. Dialogues Clin Neurosci, 11(3), 281–295. [PubMed: 19877496]

Blaszczyk JW (2018). The Emerging Role of Energy Metabolism and Neuroprotective Strategies in Parkinson's Disease. Front Aging Neurosci, 10, 301. doi:10.3389/fnagi.2018.00301 [PubMed: 30344487]

Bleau G, Chapdelaine A, & Roberts KD (1972). The assay of cholesterol sulfate in biological material by enzymatic radioisotopic displacement. Can J Biochem, 50(3), 277–286. [PubMed: 4259850]

Borowicz KK, Piskorska B, Banach M, & Czuczwar SJ (2011). Neuroprotective actions of neurosteroids. Front Endocrinol (Lausanne), 2, 50. doi:10.3389/fendo.2011.00050 [PubMed: 22649375]

Brown AM, Sickmann HM, Fosgerau K, Lund TM, Schousboe A, Waagepetersen HS, & Ransom BR (2005). Astrocyte glycogen metabolism is required for neural activity during aglycemia or intense stimulation in mouse white matter. J Neurosci Res, 79(1–2), 74–80. doi:10.1002/jnr.20335 [PubMed: 15578727]

Cai B, Li W, Mao X, Winters A, Ryou MG, Liu R,… Yang SH (2016). Neuroglobin Overexpression Inhibits AMPK Signaling and Promotes Cell Anabolism. Mol Neurobiol, 53(2), 1254–1265. doi: 10.1007/s12035-014-9077-y [PubMed: 25616953]

Charalampopoulos I, Tsatsanis C, Dermitzaki E, Alexaki VI, Castanas E, Margioris AN, & Gravanis A (2004). Dehydroepiandrosterone and allopregnanolone protect sympathoadrenal medulla cells against apoptosis via antiapoptotic Bcl-2 proteins. Proc Natl Acad Sci U S A, 101(21), 8209–8214. doi:10.1073/pnas.0306631101 [PubMed: 15148390]

Franke TF, Hornik CP, Segev L, Shostak GA, & Sugimoto C (2003). PI3K/Akt and apoptosis: size matters. Oncogene, 22(56), 8983–8998. doi:10.1038/sj.onc.1207115 [PubMed: 14663477]

Fukui M, Song JH, Choi J, Choi HJ, & Zhu BT (2009). Mechanism of glutamate-induced neurotoxicity in HT22 mouse hippocampal cells. Eur J Pharmacol, 617(1–3), 1–11. doi:10.1016/j.ejphar.2009.06.059 [PubMed: 19580806]

Grandl M, & Schmitz G (2010). Fluorescent high-content imaging allows the discrimination and quantitation of E-LDL-induced lipid droplets and Ox-LDL-generated phospholipidosis in human macrophages. Cytometry A, 77(3), 231–242. doi:10.1002/cyto.a.20828 [PubMed: 20014301]

Guo C, Sun L, Chen X, & Zhang D (2013). Oxidative stress, mitochondrial damage and neurodegenerative diseases. Neural Regen Res, 8(21), 2003–2014. doi:10.3969/j.issn.1673-5374.2013.21.009 [PubMed: 25206509]

Halim ND, McFate T, Mohyeldin A, Okagaki P, Korotchkina LG, Patel MS,… Verma A (2010). Phosphorylation status of pyruvate dehydrogenase distinguishes metabolic phenotypes of cultured rat brain astrocytes and neurons. Glia, 58(10), 1168–1176. doi:10.1002/glia.20996 [PubMed: 20544852]

Hochberg RB, Ladany S, Welch M, & Lieberman S (1974). Cholesterol and cholesterol sulfate as substrates for the adrenal side-chain cleavage enzyme. Biochemistry, 13(9), 1938–1945. [PubMed: 4152127]

Ivanisevic J, Epstein AA, Kurczy ME, Benton PH, Uritboonthai W, Fox HS,… Siuzdak G (2014). Brain region mapping using global metabolomics. Chem Biol, 21(11), 1575–1584. doi:10.1016/j.chembiol.2014.09.016 [PubMed: 25457182]

Johnson S, & Imai SI (2018). NAD (+) biosynthesis, aging, and disease. F1000Res, 7, 132. doi:10.12688/f1000research.12120.1 [PubMed: 29744033]

Lin SP, Li W, Winters A, Liu R, & Yang SH (2018). Artemisinin Prevents Glutamate-Induced Neuronal Cell Death Via Akt Pathway Activation. Front Cell Neurosci, 12, 108. doi:10.3389/fncel.2018.00108 [PubMed: 29731711]

Maragakis NJ, & Rothstein JD (2006). Mechanisms of Disease: astrocytes in neurodegenerative disease. Nat Clin Pract Neurol, 2(12), 679–689. doi:10.1038/ncpneuro0355 [PubMed: 17117171]

Murphy TH, Miyamoto M, Sastre A, Schnaar RL, & Coyle JT (1989). Glutamate toxicity in a neuronal cell line involves inhibition of cystine transport leading to oxidative stress. Neuron, 2(6), 1547–1558. [PubMed: 2576375]

Nakae H, Hiroi H, Momoeda M, Koizumi M, Iwamori M, & Taketani Y (2010). Inhibition of cell invasion and protease activity by cholesterol sulfate. Fertil Steril, 94(6), 2455–2457. doi:10.1016/j.fertnstert.2010.02.012 [PubMed: 20334863]

Nita M, & Grzybowski A (2016). The Role of the Reactive Oxygen Species and Oxidative Stress in the Pathomechanism of the Age-Related Ocular Diseases and Other Pathologies of the Anterior and Posterior Eye Segments in Adults. Oxid Med Cell Longev, 2016, 3164734. doi:10.1155/2016/3164734 [PubMed: 26881021]

Poteet E, Winters A, Yan LJ, Shufelt K, Green KN, Simpkins JW,… Yang SH (2012). Neuroprotective actions of methylene blue and its derivatives. PLoS One, 7(10), e48279. doi:10.1371/journal.pone.0048279 [PubMed: 23118969]

Prah J, Winters A, Chaudhari K, Hersh J, Liu R, & Yang SH (2019). A Novel Serum Free Primary Astrocyte Culture Method that Mimic Quiescent Astrocyte Phenotype. J Neurosci Methods. doi:10.1016/j.jneumeth.2019.03.013

Quansah E, Peelaerts W, Langston JW, Simon DK, Colca J, & Brundin P (2018). Targeting energy metabolism via the mitochondrial pyruvate carrier as a novel approach to attenuate neurodegeneration. Mol Neurodegener, 13(1), 28. doi:10.1186/s13024-018-0260-x [PubMed: 29793507]

Reynolds A, Laurie C, Mosley RL, & Gendelman HE (2007). Oxidative stress and the pathogenesis of neurodegenerative disorders. Int Rev Neurobiol, 82, 297–325. doi:10.1016/S0074-7742(07)82016-2 [PubMed: 17678968]

Roberts KD, Bandi L, Calvin HI, Drucker WD, & Lieberman S (1964). Evidence That Steroid Sulfates Serve as Biosynthetic Intermediates. Iv. Conversion of Cholesterol Sulfate in Vivo to Urinary C-19 and C-21 Steroidal Sulfates. Biochemistry, 3, 1983–1988. [PubMed: 14269322]

Roy Choudhury G, Winters A, Rich RM, Ryou MG, Gryczynski Z, Yuan F,… Liu R (2015). Methylene blue protects astrocytes against glucose oxygen deprivation by improving cellular respiration. PLoS One, 10(4), e0123096. doi:10.1371/journal.pone.0123096 [PubMed: 25848957]

Seneff S, Davidson RM, Lauritzen A, Samsel A, & Wainwright G (2015). A novel hypothesis for atherosclerosis as a cholesterol sulfate deficiency syndrome. Theor Biol Med Model, 12, 9. doi: 10.1186/s12976-015-0006-1 [PubMed: 26014131]

Shi X, Cheng Q, Xu L, Yan J, Jiang M, He J,… Xie W (2014). Cholesterol sulfate and cholesterol sulfotransferase inhibit gluconeogenesis by targeting hepatocyte nuclear factor 4alpha. Mol Cell Biol, 34(3), 485–497. doi:10.1128/MCB.01094-13 [PubMed: 24277929]

Silva RH, Abilio VC, Takatsu AL, Kameda SR, Grassl C, Chehin AB,… Frussa-Filho R (2004). Role of hippocampal oxidative stress in memory deficits induced by sleep deprivation in mice. Neuropharmacology, 46(6), 895–903. doi:10.1016/j.neuropharm.2003.11.032 [PubMed: 15033349]

Sion B, Grizard G, & Boucher D (2001). Quantitative analysis of desmosterol, cholesterol and cholesterol sulfate in semen by high-performance liquid chromatography. J Chromatogr A, 935(1–2), 259–265. [PubMed: 11762778]

Sofroniew MV, & Vinters HV (2010). Astrocytes: biology and pathology. Acta Neuropathol, 119(1), 7–35. doi:10.1007/s00401-009-0619-8 [PubMed: 20012068]

Strott CA, & Higashi Y (2003). Cholesterol sulfate in human physiology: what's it all about? J Lipid Res, 44(7), 1268–1278. doi:10.1194/jlr.R300005-JLR200 [PubMed: 12730293]

Swanson RA, & Choi DW (1993). Glial glycogen stores affect neuronal survival during glucose deprivation in vitro. J Cereb Blood Flow Metab, 13(1), 162–169. doi:10.1038/jcbfm.1993.19 [PubMed: 8417005]

Weydert CJ, & Cullen JJ (2010). Measurement of superoxide dismutase, catalase and glutathione peroxidase in cultured cells and tissue. Nat Protoc, 5(1), 51–66. doi:10.1038/nprot.2009.197 [PubMed: 20057381]

Williams ML, Hughes-Fulford M, & Elias PM (1985). Inhibition of 3-hydroxy-3-methylglutaryl coenzyme A reductase activity and sterol synthesis by cholesterol sulfate in cultured fibroblasts. Biochim Biophys Acta, 845(3), 349–357. [PubMed: 3859337]

Winter JS, & Bongiovanni AM (1968). Identification of cholesterol sulfate in urine and plasma of normal and hypercholesterolemic subjects. J Clin Endocrinol Metab, 28(6), 927–930. doi:10.1210/jcem-28-6-927 [PubMed: 5656448]

Wojtal K, Trojnar MK, & Czuczwar SJ (2006). Endogenous neuroprotective factors: neurosteroids. Pharmacol Rep, 58(3), 335–340. [PubMed: 16845207]

Yousefi B, Rastin M, Hatef MR, Shariati J, Alimohammadi R, & Mahmoudi M (2018). In vitro modulatory effect of dehydroepiandrosterone sulfate on apoptosis and expression of apoptosis-related genes in patients with systemic lupus erythematosus. J Cell Physiol. doi:10.1002/jcp.27878

Zhernova EV, & Ivanova SA (2012). [Effects of dehydroepiandrosteron sulfat on induced apoptosis of lymphocytes in healthy persons]. Fiziol Cheloveka, 38(5), 97–101. [PubMed: 23101246]

Zhou H, Li XM, Meinkoth J, & Pittman RN (2000). Akt regulates cell survival and apoptosis at a postmitochondrial level. J Cell Biol, 151(3), 483–494. [PubMed: 11062251]

Highlights

- We determined some neuroprotective effects of cholesterol sulfate.
- Cholesterol sulfate protects HT-22 cells against glutamate induced cell death.
- Cholesterol sulfate increases ATP, lipid and glycogen contents in astrocytes.
- Cholesterol sulfate activates Akt signaling and decreases AMPK phosphorylation.

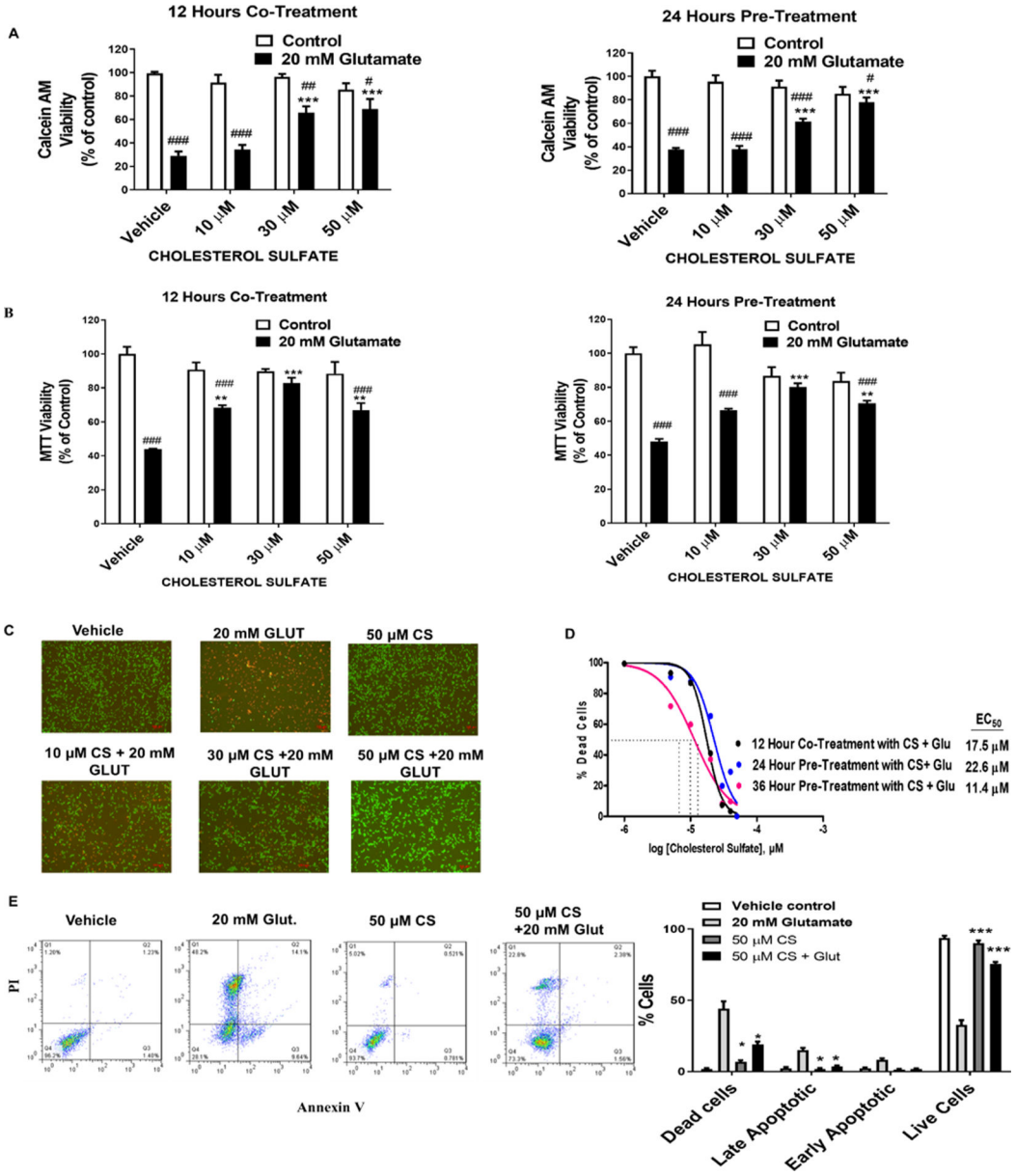

Figure 1. CS protects HT22 cells against glutamate-induced cell death.

(A) Calcien AM viability assay depicts a significant decrease cell viability after 12 hours exposure to 20 mM glutamate ($F_{1,56}$ = 145.7, $p < 0.0001$ N=6)/ ($F_{1,24}$ = 16.76, $p < 0.0001$ N=6) which was dose-dependently attenuated by CS ($F_{3,56}$ = 6.405, $p < 0.0001$ N=6)/ ($F_{3,24}$ = 5.155, $p < 0.0068$ N=6) with significant glutamate and CS interaction ($F_{3,56}$ = 11.55, $p < 0.0001$ N=6)/ ($F_{3,24}$ = 17.94, $p < 0.0001$ N=6) in the co-treatment/pre-treatment paradigm respectively. (B)) MTT viability assay depicts a significant decrease cell viability after 12 hours exposure to 20 mM glutamate ($F_{1,24}$ = 99.78, $p < 0.0001$ N=6)/ ($F_{1,24}$ = 94.54, $p < 0.0001$ N=6) which was dose-dependently attenuated by CS ($F_{3,24}$ = 4.982, $p = 0.008$ N=6)/ ($F_{3,24}$ = 3.69, $p < 0.025$ N=6) with significant glutamate and CS interaction ($F_{3,24}$ = 15.17, $p < 0.0001$ N=6)/ ($F_{3,24}$ = 14.12, $p < 0.0001$ N=6) in the co-treatment/pre-treatment paradigm respectively. (Two-way ANOVA, Bonferroni's test). *p< 0.05, **p<0.01 ***p< 0.001

compared to vehicle/glutamate, #p< 0.05, ##p<0.01 ###p< 0.001 compared to vehicle/control (C) Representative Calcein AM fluorescent images of PI (red) and Calcien AM (green) depict a dose-dependent neuroprotective effect of CS in HT-22 cells after 20 mM glutamate induce insult. (D) Dose-response curve of CS treatment of HT-22 Cells at various time points against glutamate-induced toxicity. (E) Representative flow cytometry analysis of Annexin-V and PI staining after 24 hours pre-treatment with CS. Apoptosis analysis with Two-way ANOVA, Bonferroni's test ($F_{3,32}$ = 1200, p < 0.0001) *p< 0.05, **p<0.01 ***p< 0.001 compared to 20 mM glutamate treatment (N= 4).

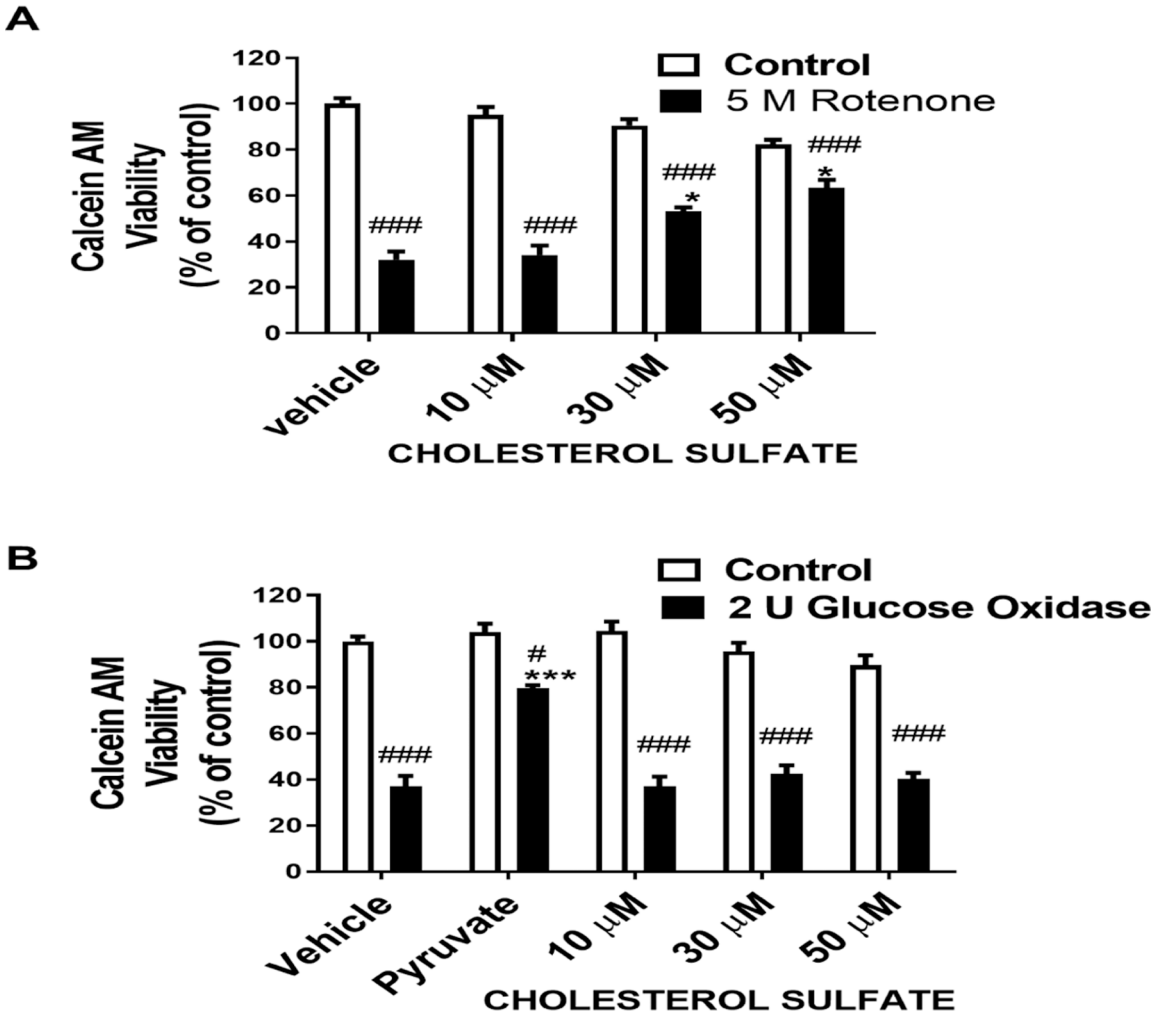

Figure 2. CS inhibited rotenone-induced neurotoxicity in HT-22.

(A) Effects of CS on rotenone-induced cell death. Cells were treated with 5 μM rotenone for 24 hours in the presence of CS. Two-way ANOVA of cell viability showed a significant rotenone and treatment interaction ($F_{3,24}$ = 26.22, p < 0.0001 N=6), a significant effect of CS treatment ($F_{3,24}$ = 3.462, p = 0.0321 N=5) and rotenone treatment ($F_{1,24}$ = 444.8, p < 0.0001 N=5) (B) 24 hours pre-treatment of HT-22 cells with CS failed to protect cells against glucose oxidase induced cell death. Two-way ANOVA of cell viability showed no significant glutamate and treatment interaction ($F_{3,24}$ = 2.604, p = 0.0753 N=6), no significant effect of CS treatment($F_{3,24}$ = 0.9114, p = 0.4502 N=6) and glucose oxidase treatment ($F_{1,24}$ = 498, p < 0.0001 N=6) *p< 0.05, **p<0.01 ***p< 0.001 compared to vehicle/glucose oxidase or rotenone, #p< 0.05, ##p<0.01 ###p< 0.001 compared to vehicle/ control

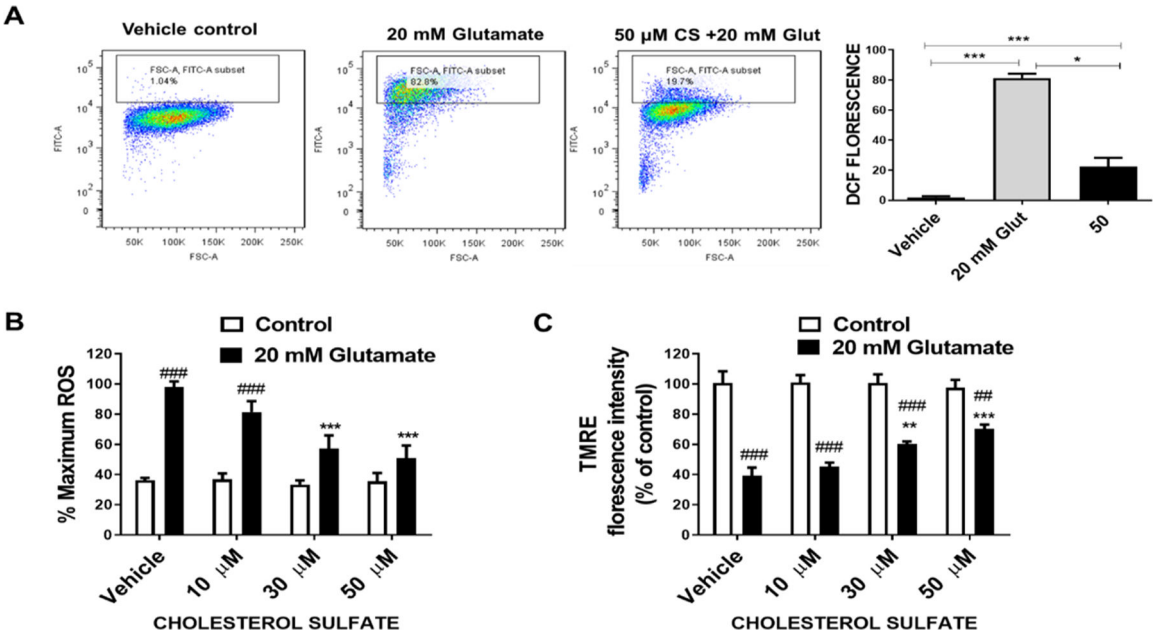

Figure 3. CS attenuates glutamate-induced ROS production and mitochondrial membrane depolarization.

(A) Representative DCF flow cytometry assay depicts a significant increase in ROS after 12 hours exposure to 20 mM glutamate which was attenuated by CS ($F_{2,6}$ = 121, p < 0.0001 N=4), (One way ANOVA and Bonferroni's test) *p< 0.05, **p<0.01 ***p< 0.001. (B) DCF microplate reader assay depicts a significant increase in ROS after 12 hours exposure to 20 mM glutamate ($F_{1,24}$ = 79.85, p < 0.0001 N=6) which was dose-dependently attenuated by CS ($F_{3,24}$ = 7.822, p = 0.0008 N=6) with significant glutamate and CS interaction ($F_{3,24}$ = 6.545, p = 0.0022 N=6). (C) TMRE plate reader assay shows CS ($F_{3,24}$ = 3.436, p = 0.0329 N=6) attenuates glutamate-induced ($F_{1,24}$ = 178.6, p < 0.0001 N=6) mitochondrial membrane potential loss with significant glutamate and CS interaction ($F_{3,24}$ = 4.988, p = 0.0079 N=6). (Two way ANOVA and Bonferroni's test) *p< 0.05, **p<0.01 ***p< 0.001 compared to vehicle/glutamate, #p< 0.05, ##p<0.01 ###p< 0.001 compared to vehicle/control

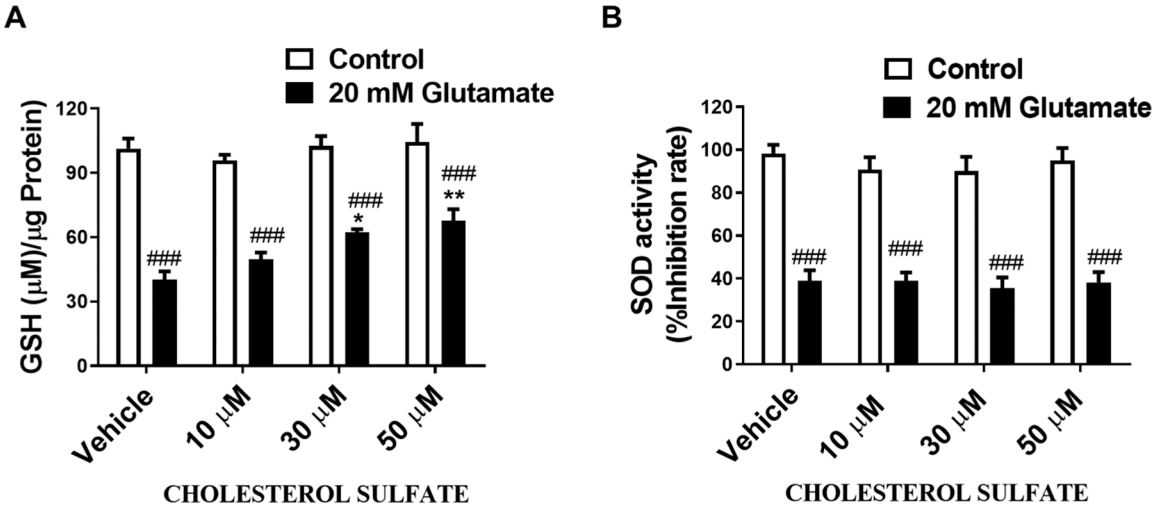

Figure 4. Pretreatment with CS prevented glutamate induced GSH depletion.

(A) Total GSH assay in HT-22 cells treated with CS and 20 mM glutamate. Glutamate induced a decrease total GSH level ($F_{1,31}$ = 185.5, p < 0.0001 N=5) which was attenuated by CS ($F_{3,31}$ = 4.636, p = 0.0086 N=5) with no significant glutamate and CS interaction ($F_{3,31}$ = 2.48, p = 0.0793 N=5) (B) Effects of CS on SOD activity following HT-22 exposure to glutamate. Glutamate induced a decrease in SOD ($F_{1,24}$ = 228.6, p = 0.001 N=5) which was not attenuated by CS ($F_{3,24}$ = 0.4638, p = 0.71 N=5) with no significant glutamate and CS interaction ($F_{3,24}$ = 0.1892, p = 0.9027 N=5) (Two way ANOVA and Bonferroni's test) *p< 0.05, **p<0.01 ***p< 0.001 compared to vehicle/glutamate, #p< 0.05, ##p<0.01 ###p< 0.001 compared to vehicle/control

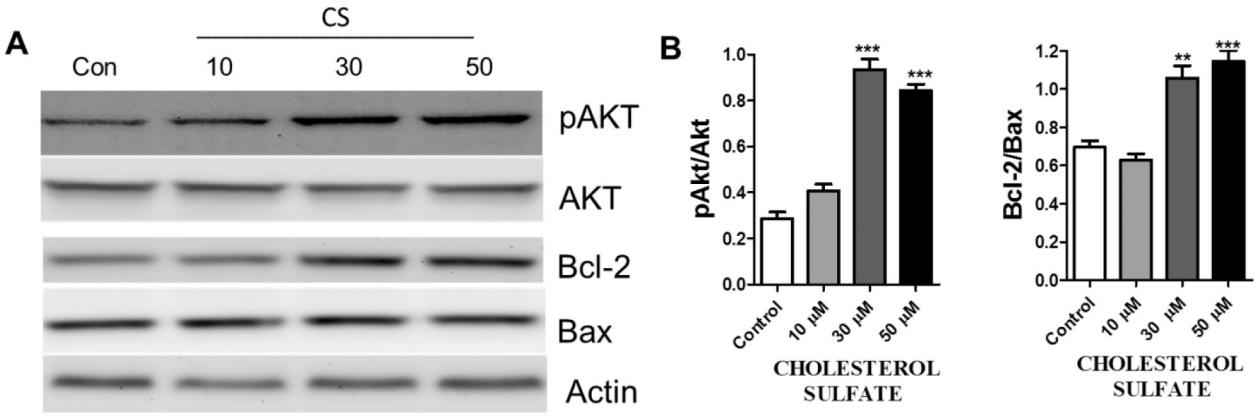

Figure 5. CS activates AKT pathway in HT-22 cells.

(A) Representative Western blots (B) Quantitative statistical analysis shows an increase in pAkt/Akt ($F_{3,12}$ = 93.27, p < 0.0001 N=4), and Bcl-2/Bax ($F_{3,12}$ = 28.62, p <0.0001 N=4), after HT-22 cells were treated with CS for 36 hours. (One way ANOVA and Bonferroni's test) *p< 0.05, **p<0.01 ***p< 0.001 compared to control.

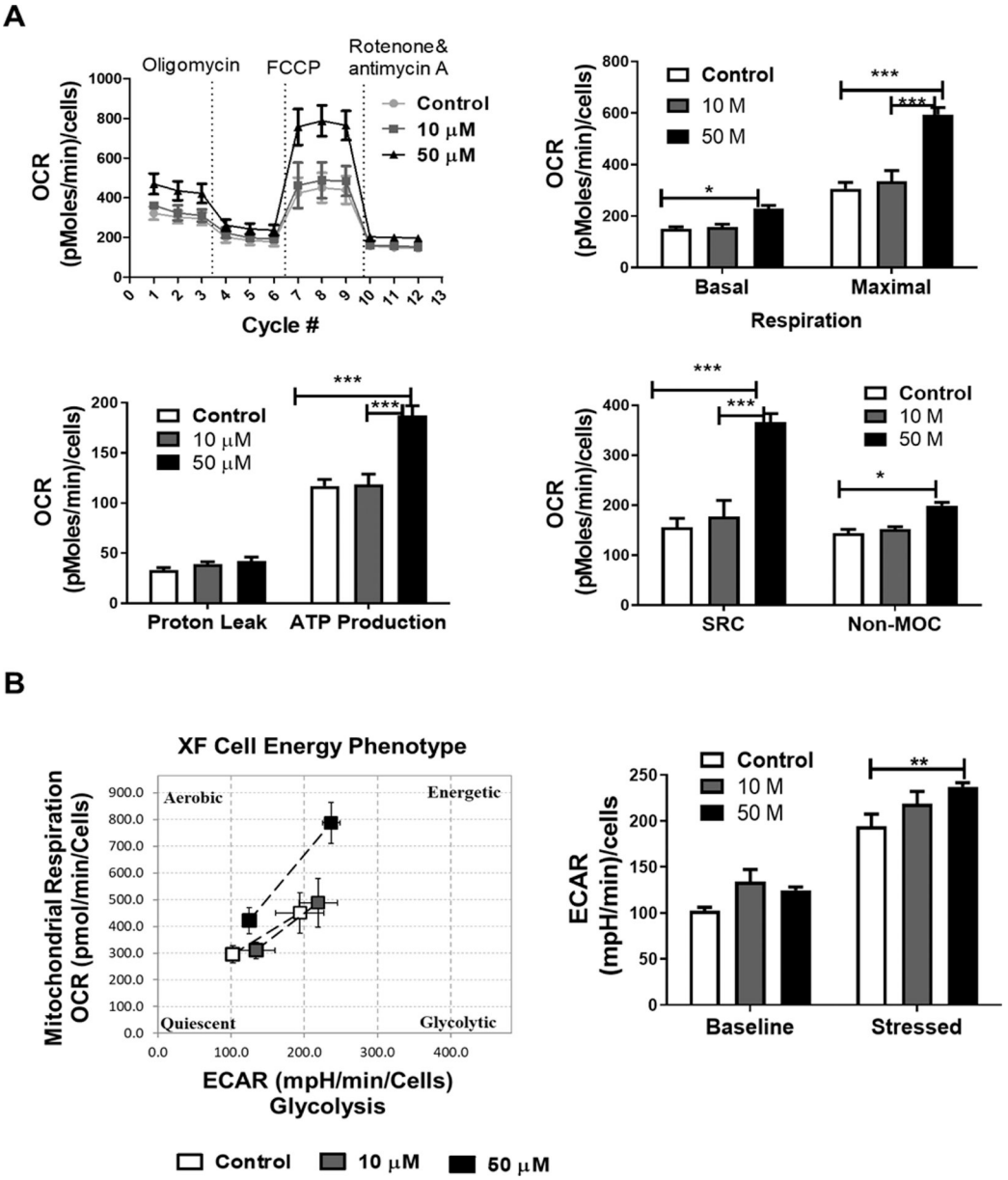

Figure 6. CS increases oxygen consumption rate (OCR) in primary astrocytes.

(A) OCR recordings at baseline and after treatment with oligomycin, FCCP and rotenone/ Antimycin A. Bar graphs indicate CS effects on basal and maximal respiration ($F_{2,30}$ = 47.10, p <0.0001), proton leak and non-mitochondrial oxygen consumption (non-MOC) ($F_{2,30}$ = 20.9, p <0.0001), as well as ATP production linked to mitochondrial respiration and spare respiratory capacity (SRC) ($F_{2,30}$ = 50.44, p <0.0001). (B) Cell energy phenotype after treatment of astrocytes with CS. Bar graph indicates the baseline and stressed extracellular acidification rate (ECAR) after CS treatment ($F_{2,30}$ = 10.01, p =0.0005). Data represented as the mean ±SEM, (Two-way ANOVA, Bonferroni's test) N= 8 per group, significance at * p< 0.05, * p< 0.01, ***p<0.001

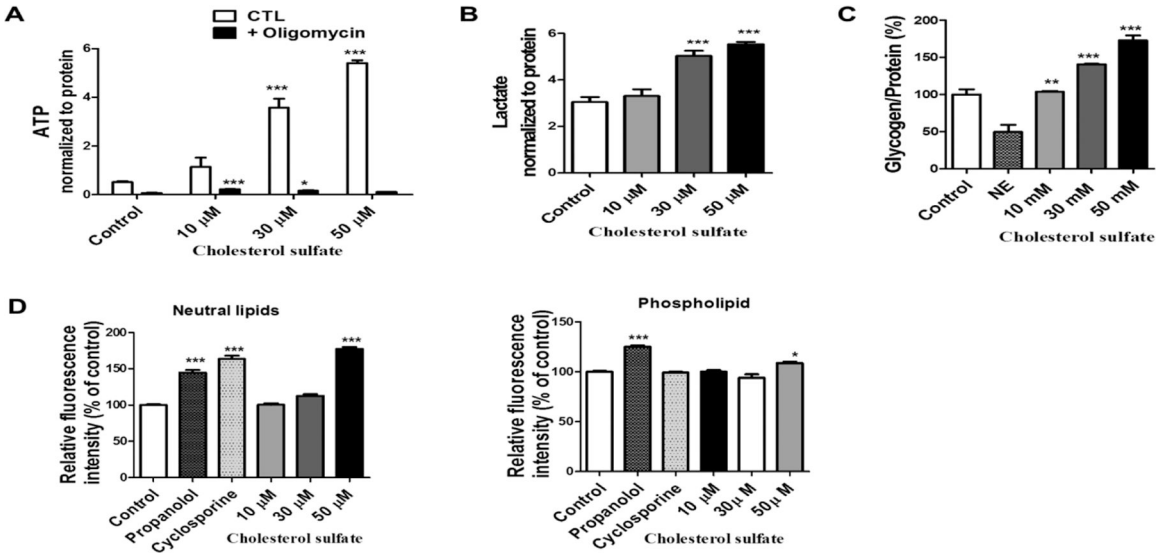

Figure 7. CS enhanced ATP production and increased glycogen content in astrocyte.

(A) Total ATP content in primary astrocytes analyzed using an ATP kit were increased in astrocytes treated with CS ($F_{3,23}$ = 61.13, p < 0.0001 N=4) and oligomycin introduction ($F_{1,23}$ = 307.83, p < 0.0001 N=4) as well as a significant oligomycin and treatment(CS) interaction ($F_{3,23}$ = 62.15, p < 0.0001 N=4). (Two way ANOVA and Bonferroni's test), significance at * p< 0.05, ** p< 0.01, ***p<0.001 vs control. (B) Lactate levels were increased in primary astrocytes treated with CS ($F_{3,28}$ = 31.83, p < 0.0001 N=8). (C) Glycogen content was increased in primary astrocytes treated with CS but not norepinephrine (NE) (decreases glycogen storage) ($F_{4,15}$ = 56.46, p < 0.0001 N=4). (D) Quantitative analysis of lipid content in astrocytes treated with CS, propranolol (induces accumulation of phospholipids) and (cyclosporine induces formation of prominent neutral lipid droplets) shows an increase in neutral lipids ($F_{5,42}$ = 131.0, p < 0.0001 N=8) and phospholipids ($F_{5,42}$ = 37.37, p < 0.0001 N=8). in astrocytes treated with propranolol, cyclosporine and 50 µM CS. (One way ANOVA and Bonferroni's test), significance at * p< 0.05, ** p< 0.01, ***p<0.001 vs control.

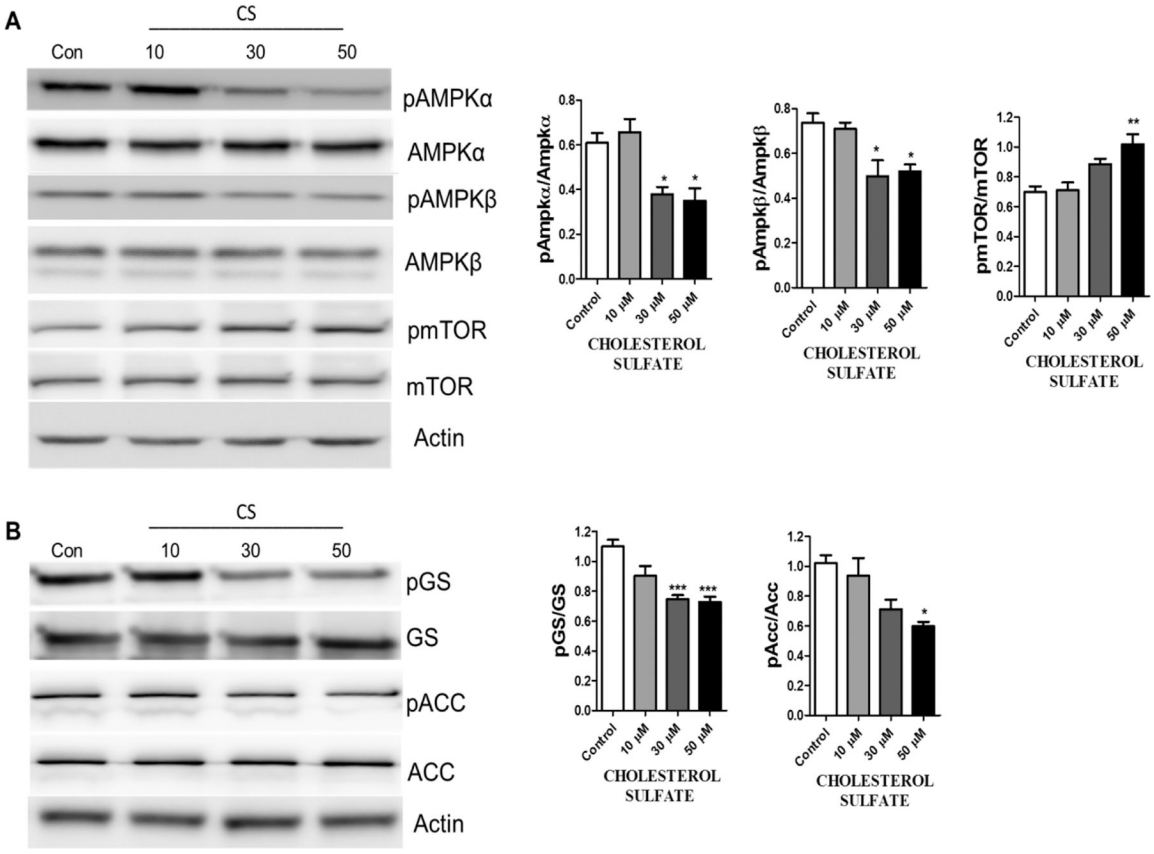

Figure 8. CS inhibits AMPK pathway in astrocytes.

(A) Representative Western blots and statistical analysis indicate a reduction in pAmpkα/Ampkα ($F_{3,12}$ = 10.15, p = 0.0013 N=4), pAmpkβ/Ampkβ ($F_{3,12}$ = 7.132, p = 0.0052 N=4), and an increase in pmTOR/mTOR ($F_{3,12}$ = 9.389, p = 0.0018 N=4), after astrocytes were treated with CS for 72 hours. (One way ANOVA and Bonferroni's test), significance at * p< 0.05, * p< 0.01, ***p<0.001 vs control. (B) Western blots and statistical analysis of GS and ACC after astrocytes were treated with CS for 72 hours indicated a reduction in p-GS/GS ($F_{3,12}$ = 14.20, p = 0.0003 N=4), and P-ACC/ACC ($F_{3,12}$ = 6.897, p = 0.0059 N=4), (One way ANOVA and Bonferroni's test), significance at * p< 0.05, ** p< 0.01, ***p<0.001 vs control.